Inverse Design of Embedded Inductor with Hierarchical Invertible Neural Transport Net

Oluwaseyi Akinwande *, Osama Waqar Bhatti*, Madhavan Swaminathan*†

*† School of Electrical and Computer Engineering † School of Material Science and Engineering

*†3D Systems Packaging Research Center, Georgia Institute of Technology, Atlanta, USA

Abstract—Heterogeneous integration of voltage regulators in power delivery networks is a growing trend that employs embedded inductor as a key component in significantly improving the power distribution. In this work, we propose a neural network framework called the hierarchical invertible neural transport for the inverse design of an embedded inductor. With this invertible method, we obtain the probability distributions of the parameters of the embedded inductor design space that most likely satisfy the desired specifications. We also learn the impedance response for free in the forward design. In the forward design, our results show a 2.14% normalized mean square error when compared with the output response of a fullwave EM simulator.

Index Terms—power delivery, inverse design, emdedded inductor, neural networks, transport maps

I. Introduction

Early-stage prototyping in electronic design automation (EDA) is often an herculean task due to a large amount of variables that are explored in the design space. The design cycle is often plagued with iterating through series of designs in an attempt to find the optimal parameters that satisfy the target specifications. These sorts of evaluations are usually compute- and time-intensive. Optimization methods and surrogate modeling have been proposed to tackle this task effectively [1]. However, the best solution may still not be obtained, or several possibilities may be ignored.

In recent times, machine learning (ML) methods have been employed to model the forward and inverse mappings for a set of inputs and outputs. Consider a design space X of a parameterized system, as illustrated in Fig. 1, that forms the input of the ML model, with corresponding output response Y. This mapping relationship can be represented as:

$$\mathcal{F}: X \to Y,\tag{1}$$

where \mathcal{F} is the forward mapping. The forward model learns the input-output relationship and predicts the output response given the input parameters. To estimate the best set of input parameters that satisfies the desired target, we find the inverse mapping:

$$\mathcal{F}^{-1}: Y \to X. \tag{2}$$

Inverse problems are often ill-posed and intractable because they fail the existence and uniqueness tests. Existence verifies if the inverse exists, and uniqueness determines the ambiguity brought by the one-to-many mapping in the inverse direction. The problem of invertibility is not novel, and several methods have been proposed to address it. In the domain of artificial neural networks, state-of-the-art generative models such as the

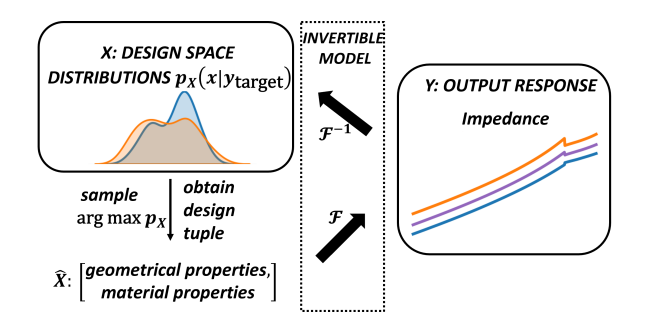


Fig. 1. Model-based invertible framework that offers a custom solution.

generative adversarial network (GAN) [2], variational autoencoder (VAE) [3], and invertible neural network (INN) [4] address this issue by generating conditional posterior distributions rather than point-estimates. In particular, the INN has some merits which include efficient computation of forward and inverse mappings, and direct modeling of its likelihood function [4].

In this paper, we propose an inverse system modeling, design and identification using hierarchical invertible neural transport net for embedded inductor in integrated voltage regulator. With inverse design, the design parameters can be straightforwardly obtained from the output objectives. It reduces design cycle time and related costs by increasing the overall efficiency of the design process. We investigate both the inverse mapping to learn the probability distributions that satisfy a desired specification, and the forward mapping to verify the solution.

II. HIERARCHICAL INVERTIBLE NEURAL TRANSPORT NETWORK (HINT)

A. Theory of Transport Maps

The theory of transport maps is based on the concept of constructing a coupling, i.e., a transport map, between a complex target probability measure ν and a simpler source probability measure μ [5]. We seek a transport map T(x) such that μ is supported on X and ν is supported on Y, i.e.,

$$T: X \to Y$$
 (3)

We can generate samples of ν by pushing forward the μ through the map. In order to conserve mass, we require [5]:

$$\mu(T^{-1}(A)) = \nu(A) \ \forall A \subset Y. \tag{4}$$

 $\mu(T^{-1}(A))$ is called the push forward of μ through T, denoted $T_{\#}\mu$. Therefore, a compact form for (4) is given as [5]:

$$T_{\#}\mu = \nu. \tag{5}$$

Choosing such a transport map involves minimizing the cost c of moving a unit of mass from x to T(x). This leads to the Monge formulation of optimal transport, given as [5]:

$$\min \left\{ \int_X c(x, T(x)) \, d\mu(x) \middle| T_\# \mu = \nu \right\}. \tag{6}$$

The solution to this constrained optimization problem is the optimal transport map. To address this problem, we pose the following questions: (1) Does the minimizer T^* exist? (2) If it exists, is it unique? (3) Is it feasible?

B. The Recursive Coupling Block

HINT uses normalizing flow based on the change-of-variables law of probabilities to model complex distributions from a simple one. The normalizing flow pipeline T is a composition of recursive coupling blocks f_i that are invertible, given as [6]:

$$T = f_{C1} \circ f_{Q1} \circ \cdots f_{CN} \circ f_{QN}, \tag{7}$$

where each pair $f_{Ci} \circ f_{Qi}$ in T is a composition of a triangular map and an orthogonal transformation, respectively, where the former is known as a Knothe-Rosenblatt rearrangement in transport maps [5]. Fig. 2 shows one such composition of a recursive affine coupling block and an orthogonal transformation. A parameterized flow model $f_{\theta i} = f_{Ci} \circ f_{Qi}$ splits the input vector x into $[x_1, x_2]$ and transforms them by an affine function with coefficients e^s and t with element-wise operations as [4]:

$$x_1' = x_1, \quad x_2' = x_2 \circ e^{s(x_1)} + t(x_1).$$
 (8)

It is easy to see that (8) is trivially invertible. This way, the inverse flow composition is easily computed as

$$T^{-1} = f_{QN}^{-1} \circ f_{CN}^{-1} \cdots \circ f_{Q1}^{-1} \circ f_{C1}^{-1}. \tag{9}$$

T in (7) is used to transport the data distribution $p_X(x)$ to a standard normal latent distribution $p_Z = \mathcal{N}(0, I)$, while T^{-1} in (9) can then be used to draw a sample $z \sim p_Z$ in the latent space to obtain p_X .

To infer the inverse solution, we can turn any z sampled from the latent space into a corresponding x conditioned on y as [6]:

$$p_X(x|y) = p_Z(f(x,y)|y) \cdot |\nabla f(x)|. \tag{10}$$

This invertible model has the benefits of efficient computation of the conditional posterior probabilities because of the dense Jacobian determinant ∇f using the recursive design, and a simpler training objective where the parameters of the flow f_{θ} can be learned from (10) via a maximum likelihood loss [6]:

$$\mathcal{L} = \frac{1}{2} \|f(x, y|\theta)\|_{2}^{2} - \log |\nabla f(x|\theta)|. \tag{11}$$

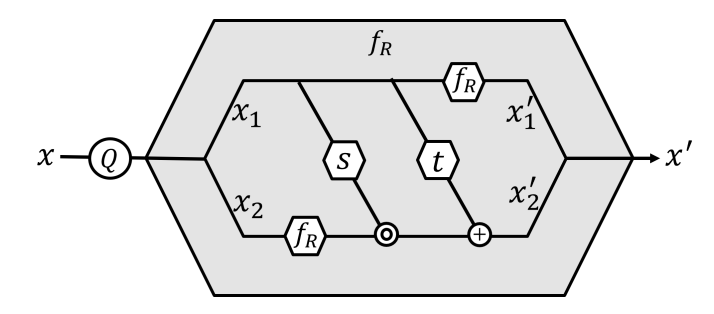


Fig. 2. A recursive affine coupling block. The inner functions f_R perform the same sequence of operations as the outer gray block, repeated until the maximum hierarchy depth is reached [6].

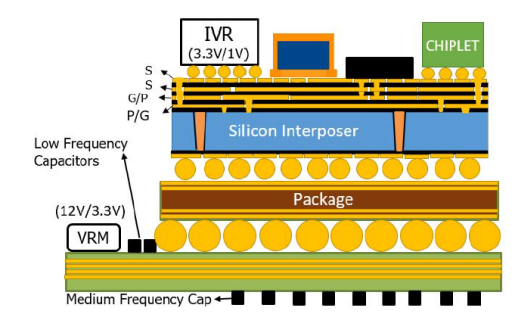


Fig. 3. Stack-up of the considered 2.5D integrated system [7].

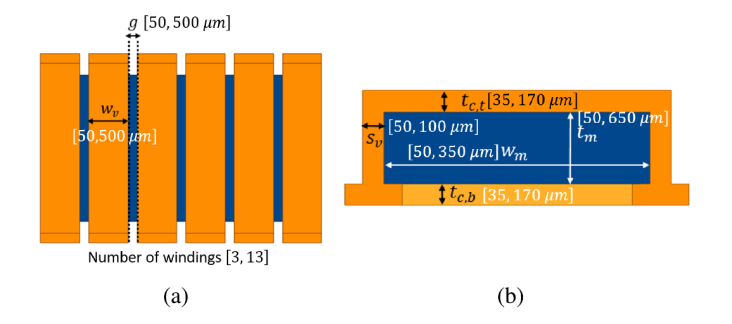


Fig. 4. Solenoid inductor [7]. (a) Top view. (b) Side view.

III. APPLICATION: INVERSE DESIGN OF EMBEDDED INDUCTOR

For a demonstration of the proposed method, we apply the HINT method for the inverse design of an embedded solenoidal inductor. The inductor is made up of a Nickel-Zinc (NiZn) ferrite magnetic core and it is integrated on the top metal layer of a silicon-interposer-based 2.5D heterogeneously integrated system as in Fig. 3 [7]. The output response of the solenoidal inductor is the impedance $Z = \mathrm{ESR} + j\omega L$, where L is its inductance and and ESR is its equivalent series resistance. The objective here is to (1) obtain the solenoidal inductor design parameters that correspond to a given specification of impedance response Z, and (2) validate the design parameters through a forward evaluation.

A. Model Setup

The design parameters of the solenoidal inductor and their range of values are shown in Fig. 4. The target characteristic

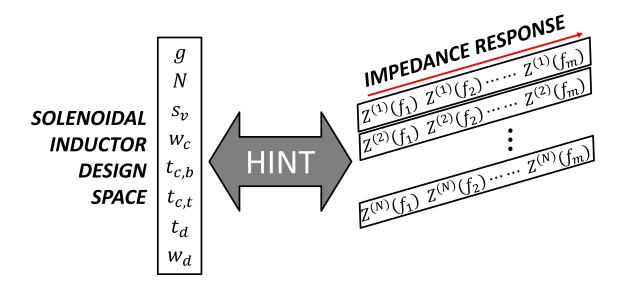


Fig. 5. Proposed Hierarchical Invertible Neural Transport (HINT) model setup for embedded inductor.

investigated is the impedance response Z with the frequency being swept from 15-98 MHz for 34 frequency points. Using Latin Hypercube Sampling, we determine 949 samples and extract their inductance and ESR with Ansys HFSS. We split the data into train and test sets.

The objective here is to determine an invertible mapping between the design space X and output response Y. The proposed model setup is shown in Fig. 5. The HINT model is constructed using 2 recursive coupling blocks with 3 recursion levels. Each recursive block contains the scale s and shift t networks which are constructed with fully connected neural networks with one hidden layer of 256 neurons, Rectified Linear Unit (ReLU) activation functions, and batch normalization layers. On the input side of the model setup, there are 8 inductor design parameters. The output variable is the impedance response Z. The HINT model is trained for 500 epochs.

B. Results

During the inference process, we choose a random response $y_{\rm target}$ from the test set and we obtain the inverse solution using (10). The HINT model generates rich conditional posterior distributions of the embedded inductor design parameters as shown in Fig. 6. Next, we obtain an inverse tuple from these distributions by sampling the points with the highest densities in the embedded inductor design space. The tuple obtained is $\{128.7~\mu\text{m}, 499~\mu\text{m}, 109.8~\mu\text{m}, 145.2~\mu\text{m}, 303~\mu\text{m}, 10.7~\text{mil}, 8.2~\text{mil}, 9\}$. We take this tuple and perform a forward evaluation with the HINT model to obtain the impedance response shown in Fig. 7. In the forward design, we achieve a 2.14% normalized mean square error, averaged over 10 inference runs.

IV. CONCLUSION

We present the HINT method for the inverse design of embedded inductor for integrated voltage regulator. We applied this method to obtain the probability distributions of the inverse solutions that satisfy target specifications.

ACKNOWLEDGMENT

This material is based upon work supported by the National Science Foundation under Grant No. CNS 16-2137259 - Center for Advanced Electronics through Machine Learning (CAEML).

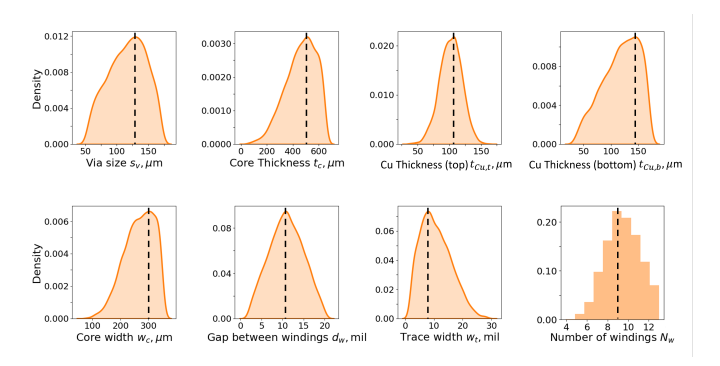


Fig. 6. Predicted conditional posterior distributions $p(x|y_{\text{target}})$ of embedded inductor design parameters. Black vertical dashed lines indicate the points with the highest densities. When the points corresponding to the highest densities are sampled for the design parameters, the tuple obtained is $\{128.7 \ \mu\text{m}, 499 \ \mu\text{m}, 109.8 \ \mu\text{m}, 145.2 \ \mu\text{m}, 303 \ \mu\text{m}, 10.7 \ \text{mil}, 8.2 \ \text{mil}, 9\}$.

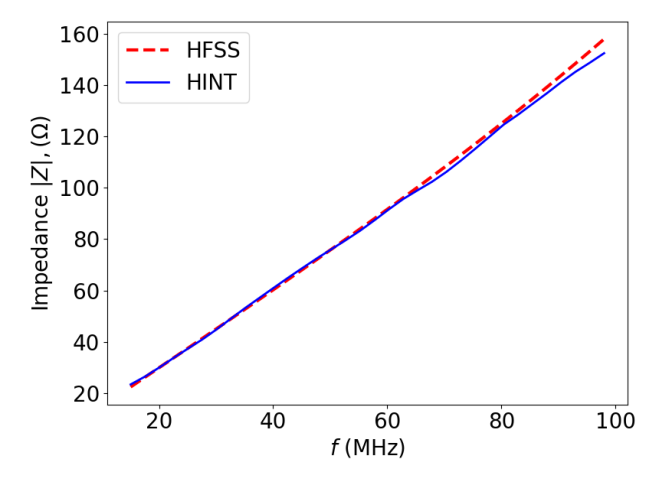


Fig. 7. Forward evaluation, showing impedance response for the embedded inductor, with HFSS and the trained HINT model for generated tuple $\widehat{x} \sim p(x|y_{\text{target}})$.

REFERENCES

- [1] M. Swaminathan, H. M. Torun, H. Yu, J. A. Hejase and W. D. Becker, "Demystifying Machine Learning for Signal and Power Integrity Problems in Packaging," in IEEE Transactions on Components, Packaging and Manufacturing Technology, vol. 10, no. 8, pp. 1276-1295, Aug. 2020, doi: 10.1109/TCPMT.2020.3011910.
- [2] Ian Goodfellow et al., "Generative Adversarial Nets", in Advances in Neural Information Processing Systems 27 (NeurIPS) 2014.
- [3] Diederik P Kingma and Max Welling. Auto-encoding variational bayes. arXiv preprint arXiv:1312.6114, 2013
- [4] Lynton Ardizzone, Jakob Kruse, Carsten Rother, Ullrich Köthe, "Analyzing Inverse Problems with Invertible Neural Networks", International Conference on Learning Representations (ICLR) 2019.
- [5] Y. Marzouk, et al., "Sampling via measure transport: An introduction". In R. Ghanem, D. Higdon, and H. Owhadi, eds., "Handbook of Uncertainty Quantification", 1–41, Springer, 2016.
- [6] Kruse, Jakob et al., "HINT: Hierarchical Invertible Neural Transport for Density Estimation and Bayesian Inference," arXiv, 2021, doi:10.48550/ARXIV.1905.10687.
- [7] H. M. Torun et al., "A Spectral Convolutional Net for Co-Optimization of Integrated Voltage Regulators and Embedded Inductors," 2019 IEEE/ACM International Conference on Computer-Aided Design.